Journal of Polymer Research (2020) 27:48
https://doi.org/10.1007/s10965-020-2022-z

ORIGINAL PAPER

Polypyrrole inter-layered low temperature curing benzoxazine matrices with enhanced thermal and dielectric properties

P. Prabunathan [1] · A. Vasanthakumar [1] · M. Manoj [1] · A. Hariharan [1] · M. Alagar [1]

Received: 24 July 2019 / Accepted: 29 January 2020

Abstract

In the present work, curing reaction of benzoxazine was studied with the incorporation of different weight percentage of polypyrrole (PPy). Conventional benzoxazine derived from Bisphenol-F, aniline (BF-a) and bio-based benzoxazine derived from cardanol, furfurylamine (C-f) were synthesized and studied. Significant change in curing temperature (Tp) was observed with the addition of PPy to both C-f and BF-a monomers. With the incorporation of 5 wt% PPy, the Tp of C-f significantly reduced from 245 °C to 185 °C and similarly for BF-a monomer from 226 °C to 165 °C. The plausible mechanism of the benzoxazine ring opening reaction in presence of PPy is also discussed. Further, scanning electron microscopy (SEM) and X-ray diffraction studies suggest that the incorporation of PPy leads to the formation of fractal morphology. Consequently, the PPy inter-layered poly(C-f) and poly(BF-a) matrices contribute to the achievement of low value of dielectric constant (K = 3.39 and 3.83). In addition, PPy interlayer provokes enhanced thermal stability and higher LOI value. Thus, the present work demonstrates the catalytic role of PPy towards the curing reaction of benzoxazines and its contribution towards thermal and dielectric behaviour the of resulted matrices.

Keywords Benzoxazines · Polypyrrole · Catalyst · Low temperature cure · Thermal properties

Introduction

Polybenzoxazine (PBZ) has emerged as a novel class of alternative phenolic thermoset material that replaces traditional epoxy, phenolic and bismaleimide matrices [1–4]. Polybenzoxazine receives much attention from both academic and industrial perceptive because of their useful high performance properties such as excellent mechanical, electrical, and chemical resistant behaviour as well as ease of processability, low out gassing and shrinkage on curing [1, 5–11]. Unfortunately, most of the developed benzoxazine monomers require high temperature curing (Tp > 200 °C) [12]. For examples, i) curing reaction of conventional benzoxazine derived from bis-phenol-F, and aniline requires temperature greater than 225 °C [13, 14], ii) low cost bio-benzoxazines derived cardanol and furfuryl amine requires temperature higher than 240 °C [15, 16].

The inadequacy associated with the curing can be alleviated through the process of i) addition of catalyst and ii) building polar functional groups on the monomers [17, 18] Designing monomers with polar functional groups to reduce curing temperature often need industrially insignificant harsh reaction condition, high cost precursors. Meanwhile, several catalysts such as organic compounds (toluene sulfonates, diamines, thiols) and Lewis acids (PCl_5, $POCl_3$, $TiCl_4$, $AlCl_3$, $FeCl_3$) were significantly employed to achieve low temperature curing [3, 19]. However, addition of such catalysts results in high viscosity, which in turn drops the shelf life in practical use. Hence, the development of catalytic system that cure benzoxazines without altering the in-built properties of the resulted matrices is highly warranted.

Recently, various amines were used as efficient catalyst to lower the curing temperature of benzoxazines [7, 12, 17, 20–22]. For example, Sun et al. performed the curing of BA-a and BF-a monomers at 150 °C with the addition of various commercially available amines [23]. Recently, Li

Electronic supplementary material The online version of this article (https://doi.org/10.1007/s10965-020-2022-z) contains supplementary material, which is available to authorized users.

✉ P. Prabunathan
nanonathan@gmail.com

✉ M. Alagar
mkalagar@yahoo.com

[1] Polymer Engineering Laboratory, PSG Institute of Technology and Applied Research, Coimbatore 641062, India

Published online: 05 February 2020

et al. 2017 prepared aniline-dimer-based benzoxazine (BA–PADPA), whose polymerization temperature was found to be low (Tp = 161 °C) [24]. Subsequently, few other research groups also studied benzoxazine ring opening reactions using primary amines, secondary amines and amine salts [17, 22, 25]. Zhang et al. 2017 developed a *m*-phenylenediamine formaldehyde oligomer and used as accelerator to cure of benzoxazine resin at 215 °C [20].

Therefore, numerous researches are in progress towards exploring the catalytic role of different amines. Further, the amide group are found to be inevitable in curing of benzoxazine rings [24, 26]. For examples, Agag et al. 2010 reported the amide linkage assisted low temperature curing benzoxazine [22]. Recently, *o*-trifluoroacetamide functional benzoxazine was prepared by Zhang et al. 2017, which also performed as a latent catalyst [27]. However, no significant attention has been focused on the role of amine group present in heterocyclic scaffold. Polypyrrole (PPy) is well known conductive polymer with conjugated heterocyclic five membered ring holding a secondary amine. Because of its easy synthesis, high conductivity, excellent stability, low-cost and high yield, great attention has been focused on the polymer [28, 29].

Till date there are no reports for the utilization of PPy as a catalyst to achieve low temperature cure benzoxazines. Inspired from amine catalyzed curing mechanism and our continuing interest in benzoxazine chemistry made us to study the present work. Thus, the effectiveness of secondary amine present in the polypyrrole has been studied towards the curing of benzoxazines. In the present work, curing behaviour of conventional bisphenol-F and bio-source cardanol based benzoxazine monomers were studied in the presence of different weight percentages of PPy. The resulted matrices were studied for their thermal and electrical properties and the data obtained are discussed and reported.

Experimental

Materials

Bisphenol-F was received from Anabond R&D, Chennai, India. Cardanol was purchased from Satya Cashew Products, Chennai. India. Pyrrole, furfuryl amine, aniline, and formaldehyde were obtained from SRL Pvt. Ltd. India. Chloroform, sodium hydroxide, ammonium persulphate, hydrochloric acid and tetrahydrofuran were obtained from Merck, India.

Preparation of Polypyrrole (PPy) and benzoxazine monomers

PPy was prepared as per the procedure reported in literature [30, 31]. 1 mL of freshly distilled pyrrole monomer was dissolved in 50 mL of 1 M HCl and sonicated for 30 min. To this mixture, the required amount of homogeneous solution of ammonium per sulphate was dissolved in 50 mL of hydrochloric acid (1 M) and was slowly added with continuous stirring for another 5 h at 0–5 °C in an ice bath. Then, the resulted black coloured product was washed several times with 1 M HCl and dried in hot air oven at 60 °C and preserved. Bio-benzoxazine (C-f) was prepared using stoichiometric quantities of cardanol, furfuryl, and formaldehyde (1:1:2) through Mannich reaction [32]. Conventional benzoxazine (BF-a) monomer was prepared using Bisphenol-F, aniline and formaldehyde in stoichiometric quantities (2:1:4) as per the reported procedure. [33]

Preparation of PPy incorporated PBz matrices

Benzoxazine monomers (BF-a and C-f) and different weight percentages of PPy (0, 1.0, 2.0, 3.0, 4.0 & 5.0 wt%) were separately added in 10 ml of THF and subjected to ultrasoniation for 2 h to obtain homogeneous distribution of PPy. The resulted solution was then poured into respective silane-coated glass plates and allowed to evaporate at room temperature for 8 h. The polymerization was initiated via stepwise thermal curing (120 °C, 160 °C, 200 °C, and 240 °C for 2 h respectively) to obtain the corresponding PPy/poly(BF-a) and PPy/poly(C-f) matrices. The formation PPy/poly(C-f) matrix is presented in Scheme 1.

Characterization

Fourier transform infrared (FT-IR) spectra were recorded on Thermo scientific Nicolet 6700-FTIR spectrometer. NMR spectra were obtained with Bruker (400 MHz) using dimethylsulfoxide (d6-DMSO) as a solvent and tetramethylsilane (TMS) as an internal standard. The curing temperature of the monomers as well as thermal stability of the matrices were determined using TGA-DSC NETZSCH STA 449F3 Jupiter -German under N_2 purge (60 mL min^{-1}) at scanning rate of 10 °C min^{-1}. X-Ray diffraction patterns were recorded at room temperature, by monitoring the diffraction angle 2θ from 10 to 80° on a PANalytical X'pert3 powder, the Netherlands. The morphology of the matrices were identified from an FEI QUANTA 200F highresolution scanning electron microscope (HRSEM). The dielectric constant was determined from LCR meter (NumetriQ, PSM – 1735, UK) at room temperature using platinum electrode from 1 Hz to 1 MHz.

Results and discussion

Structural analysis

The BF–a and C-f monomers were prepared and their molecular structures are confirmed through spectral studies such as

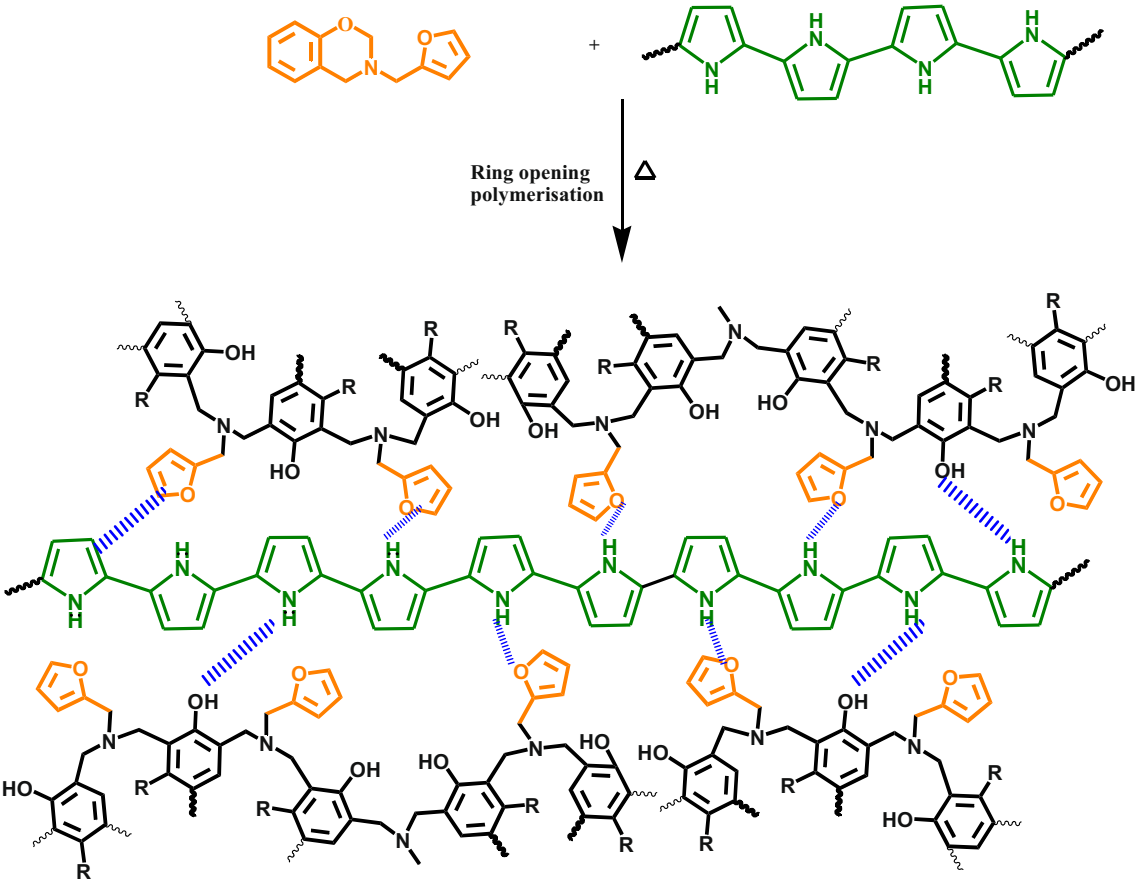

Scheme 1 Schematic representation of the formation of PPy inter-layered poly(C-f) matrix

NMR and FTIR spectroscopy. The ^{1}H NMR spectra of (C-f) and (BF-a) monomers are presented in Fig. 1a and b respectively. The ^{13}C-NMR spectra of (C-f) and (BF-a) monomers are presented in Figs. S1a and S1b (supporting information) respectively. The appearance of two singlets correspond to the methylene protons of (-O-CH_2-N-) and –N-CH_2-Ar) are used to validate the formation of the benzoxazine monomer. With respect to nature of precursors, the positions of the peaks correspond to methylene protons show minor shifts [32–34] .

In the case of C-f, two singlet signals at δ 3.9 and δ 4.9 ppm corresponds to the presence of methylene protons of oxazine rings. In addition third singlet signal at δ 3.8 corresponds to the methylene protons of furfural moiety. Moreover, the terminal methyl protons of cardanol moiety appeared at δ 0.8 ppm. The major signals appeared between δ 1.0 and 2.0 ppm corresponds to aliphatic chain protons of cardanol moiety. The multiplet signals appeared around δ 6.5–7.2 corresponds to the aryl rings. In addition,

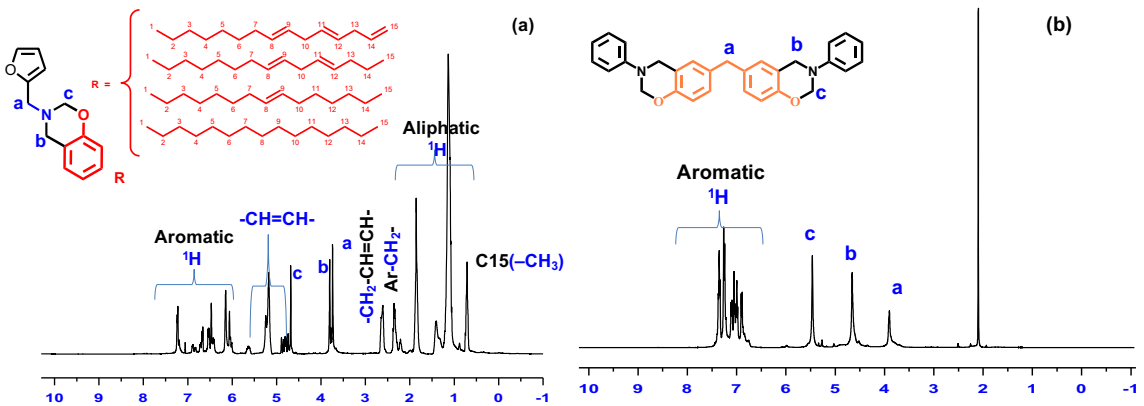

Fig. 1 ^{1}H-spectra of (**a**) C-f and (**b**) BF-a monomers

the signals appeared at δ 2.4 and 3.6 correspond to the protons of unsaturated carbon present in cardanol. This confirms that the cardanol has mixture of isomers. The ^{1}H NMR spectrum of pure cardanol is also shown in Fig. S2 (supporting information) with similar signals. On the other hand, the BF-a benzoxazine shows three major singlet signals in Fig. 1b. The two signals observed at δ 4.5 and δ 5.5 ppm correspond to the methylene protons of (-O-CH_2-N-) and –N-CH_2-Ar) oxazine rings. Further, the singlet signal appeared at δ 3.9 corresponds to the methylene group that bridges the two benzene rings of bisphenol-F. Thus, the NMR observations clearly demonstrated the formation of benzoxazines. Further, ^{13}C spectra of both monomers were presented in Fig(s). S1a-b. The spectrum of C-f (Fig. S1a) showed two signals at δ 51 and δ 80 ppm, which represents the methylene carbons of benzoxazine ring, whereas that of methylene carbon of the BF-a moiety (Fig. S1b) shows signals at δ 60 and 80 ppm. The quaternary carbon of benzoxazine ring adjacent to oxygen atom appeared in deshielding region at δ 152 ppm in both molecules. The observed chemical shift values are in accordance with those of previous reports [23, 32].

The FTIR spectra of both the monomers (C-f and BF-a) are presented in Fig. 2a along with PPy. The formations of benzoxazines are confirmed through out-of-plane C-H stretching of benzene ring attached to oxazine. Both monomers (C-f and BF-a) clearly exhibits out-of-plane C-H stretching vibration bands at 935 and 949 cm^{-1} respectively [35, 36]. The bands appeared at 1229 and 1033 cm^{-1} correspond to asymmetric and symmetrical C–O–C stretching, respectively. The bands observed at 811 cm^{-1} of C-f and 820 cm^{-1} of BF-a, corresponds to the asymmetric stretching vibration of C–N–C groups. Furthermore, the strong peaks appeared at 2924 and 2846 cm^{-1} for C-f monomer corresponds to the respective symmetric and asymmetric stretching of aliphatic –CH_2- groups of cardanol side chain. In addition, the bands appeared at 1501 cm^{-1} of BF-a and 1494 cm^{-1} of C-f corresponds to the stretching vibrations of trisubstituted benzene rings of both monomers, respectively. Further, the appearance of bands at 1590 cm^{-1} and 1285 cm^{-1} are contributed by the vibrations of furan ring present in the monomer [36, 37]. Thus, the vibration spectra confirms the formation of benzoxazine monomers.

The FTIR spectrum of polypyrrole (PPy) was also presented in Fig. 2a. The occurrence of bands at 1457 cm^{-1} and 1290 cm^{-1} correspond to the in plane deformation and stretching vibrations of C-N bond respectively. The appearance of peaks at 1044 and 914 cm^{-1} correspond to the = C-H of polypyrrole as in accordance with previous report [38]. Further the bands appeared at 1543 cm^{-1} corresponds to the vibration of C=C bond of the pyrrole rings. In addition, the formation of polybenzoxazine matrices in presence of PPy were also studied using FTIR and morphological studies.

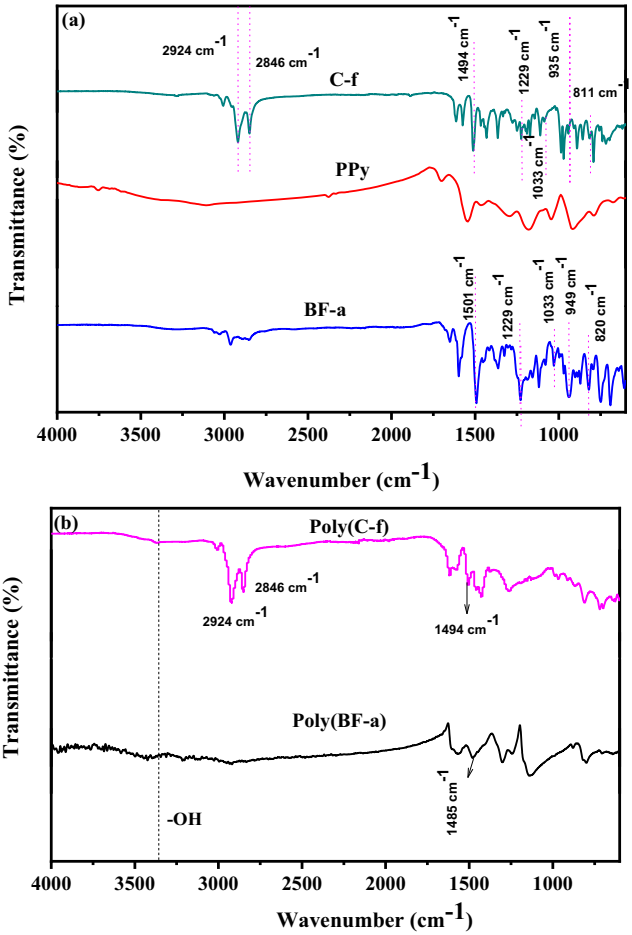

Fig. 2 FTIR spectra of (**a**) monomers (C-f, BF-a), PPy, and (**b**) neat poly(C-f) and poly(BF-a) matrices

Curing behaviour

The curing reaction of both monomers C-f and BF-a were studied using DSC. The observed thermograms obtained are presented in Fig. 3a and b respectively. In addition, the curing behaviours were presented in Table 1. The curing onset of C-f monomer begins at 220 °C and completes at 268 °C (Fig. 3a), whereas the BF-a onset begins at 200 °C and completes at 263 °C (Fig. 3b). The appearance of single exothermic peaks at 249 °C for C-f (Fig. 3a) and at 228 °C for BF-a (Fig. 3b) confirms the ring opening polymerization as presented in Scheme 2. Consequently, the tri-substituted benzene ring became tetra-substituted, which results in the formation of three-dimensional benzoxazines matrices.

The high temperature requirement for curing is the major difficulty associated with benzoxazines monomers. Earlier reports suggest that amine derivatives are good enough to provide low curing temperature for benzoxazine through their catalytic behaviour [12, 20, 21, 35]. Hence, the curing processes of both monomers are studied in the presence of nitrogen rich conductive PPy in different percentage for the first time. The observed thermograms are also presented in the

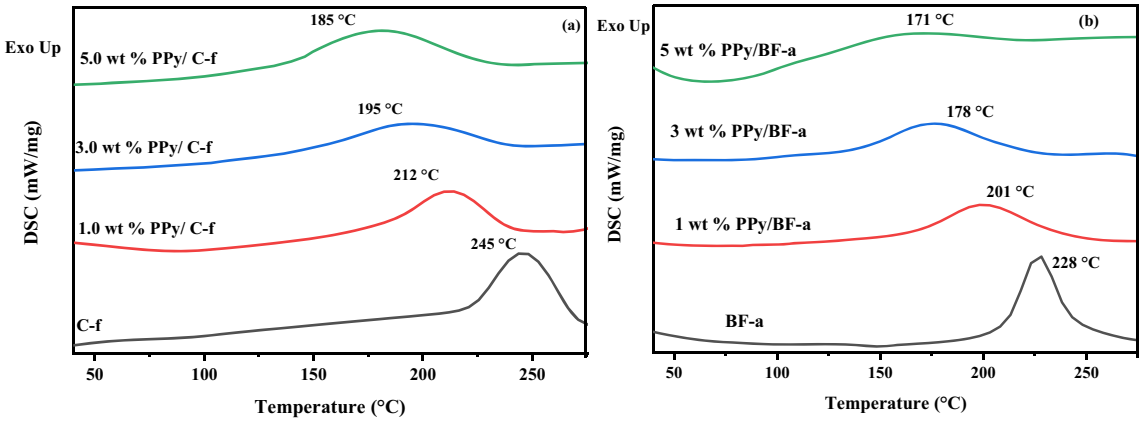

Fig. 3 DSC thermograms of (**a**) PPy/(C-f) and (**b**) PPy/(BF-a)

Fig(s). 3a and b. As expected, the polymerization of both the monomers were occurred significantly at lower temperatures (Tp). Further, the appearance of single exothermic peaks even after the addition of PPy, suggest that the curing occurs in a single step.

Addition of 5 wt% of PPy offers lower temperatures curing, beyond which no significant change in the curing temperatures were observed. Accordingly, Tp of C-f and BF-a in the presence of 5 wt% are observed at 185 °C (Fig. 3a, Table 1) and 165 °C (Fig. 3b, Table 1) respectively. Further, notable changes in the onset of curing temperatures are also observed. The C-f shows the onset at 130 °C (Fig. 3a, Table 1), whereas that of B-F shows at 123 °C (Fig. 3b, Table 1). The significant low curing temperatures observed in the present work are in accordance with those of various types of amines used to cure benzoxazines [17, 19, 20, 24, 25]. Thus, similar to oligomeric amines [20], primary amine [23], and amide [22, 27], the polypyrrole with secondary amine on five membered hetero rings is also capable of reducing the curing temperature of benzoxazines.

Meanwhile, during the curing processes the values of change in enthalpy (ΔH) are observed to decrease with the addition of PPy (Table 1). This phenomenon suggests that the PPy has a capability to reduce the exothermic nature of polymerization process through the formation of low energy activation path. This observed behaviour is in accordance with those of earlier reports, which also delivers lower enthalpy during curing reaction in the presence of different amine catalysts [20, 25, 33]. In addition, present work explores the potential usage of PPy with a series of secondary amines in five membered ring to reduce the curing temperature relatively at lower enthalpy. Thus, observations made in the present work will provide significant outcome in the field of benzoxazine chemistry. The appropriate mechanism involving the curing behaviour assisted by PPy in comparison with polyindole is discussed separately.

The curing of benzoxazines and formation of polybenzoxazine matrices are studied through FTIR and resulted spectra are presented in Fig. 2b. After thermal curing the disappearance of the bands at 935and 949 cm^{-1} for C-f and BF-a confirms the occurence of ring opening polymerization of the benzoxazine monomers, which in turn forms the poly(C-f) and poly(BF-a) matrices respectively. In addition, it is observed that the peaks corresponding to trisubstituted benzene rings at 1494 and 1501 cm^{-1} are also disappeared. Further, the new bands appeared at 1494 cm^{-1} of poly(C-f) and 1485 cm^{-1} of poly(BF-a) corresponds to the formation of tetrasubstituted benzene rings, during curing of monomers [37]. The appearance of broad bands around 3350 cm^{-1} are ascertained for the strong overlapping signals for intramolecular and intermolecular interaction of OH with O and N through hydrogen bonding, which occurred after curing [39].

Table 1 Curing characteristics of cardanol and bis-phenol-F monomers with different wt% of PPy

Monomers	PPy (Wt%)	Peak Maximum (T_P) (°C)	Curing Temperature Window (°C)	Enthalpy, (ΔH) (J/g)
C-f	0	245	220–268	127
	1	212	172–239	115
	3	195	150–237	94
	5	185	130–228	37
BF-a	0	226	200–263	116
	1	201	161–244	74
	3	178	135–227	56
	5	165	123–202	33

Figures 4 and 5 show the FT-IR spectra of the PPy/poly(C-f) and PPy/poly(BF-a) respectively. As discussed in Fig. 2b, the absence of bands at 935 cm^{-1} (Fig. 4) and at 949 cm^{-1} (Fig. 5), confirms the ring opening polymerization of the benzoxazines after addition of PPy. In Fig(s). 4 and 5, the disappearance of bands at 1494 and 1501 cm^{-1} confirms the formation of tetrasubstituted benzene rings. As a result, new band appears at 1501 cm^{-1} (Fig. 4) and 1485 cm^{-1} (Fig. 5) corresponds to the tetrasubstituted benzene rings of poly(C-f) and poly(BF-a) matrices respectively. The band appeared at 1260 cm^{-1} corresponds to the C-O-C stretching vibration. Thus, the formation polybenzoxazine matrices have been confirmed post to the addition of PPy.

Mechanism of PPy assisted curing reaction

The general mechanism corresponding to the ring opening polymerization of benzoxazines is presented in Scheme 2, which usually requires high temperature. In presence of polypyrrole curing temperature of the benzoxazines were noticed to decrease, which might be due to the catalytic nature of polypyrrole. A plausible mechanism for the catalytic action of polypyrrole is shown in Scheme 3. The lone pair on the nitrogen atom of the polypyrrole ring on heating initiates the ring opening of benzoxazine moieties to achieve the intermediate-I (In-1). Intermediate-1 can further undergo through two pathways either 'a' or 'b'. In the pathway a, the highly feasible migration of the lone pair on the tertiary nitrogen followed by a prototropic shift results in the formation of Zwitter ion (iminium nitrogen cation and a secondary carbanion) and regenerates the polypyrrole is proposed. Further, the secondary carbanion of the Zwitter ion attacks the iminium nitrogen cation of another Zwitter ion as a chain reaction followed by keto-enol tautomerism ends up in the polybenzoxazine network with polypyrrole stacking in between them.

However, in pathway 'b', the less feasible migration of the lone pair on the nitrogen atom of the pyrrole moiety could only result in the formation of unstable methylene pyrrolium cation. The above explanation obviously rules out the pathway 'b' mechanism and hence pathway a mechanism can only explain the catalytic activity of the regenerated polypyrrole.

Further, in order to ascertain the catalytic behaviour of PPy, 5 wt% polyindole was incorporated with both the benzoxazine monomers and their curing behaviour was studied. The obtained data are presented in the Fig. S3. It was interesting to note that the addition of polyindole doesn't yield any significant contribution in reducing the curing temperature as PPy. It was observed that, the 5 wt% polyindole incorporated poly(C-f) and poly(BF-a) shows only Tp value as 228 °C and 202 °C respectively. This phenomenon shows that addition of polypyrrole with benzoxazines comparatively reduces the curing temperature than that of polyindole (PI), though both have similar pKa values. It is expected that the linear and amorphous nature of PPy (Fig. 7) favours interaction with benzoxazine monomers. However, the PI was found to have nonlinear and crystalline morphology (Fig. S4). Because of the

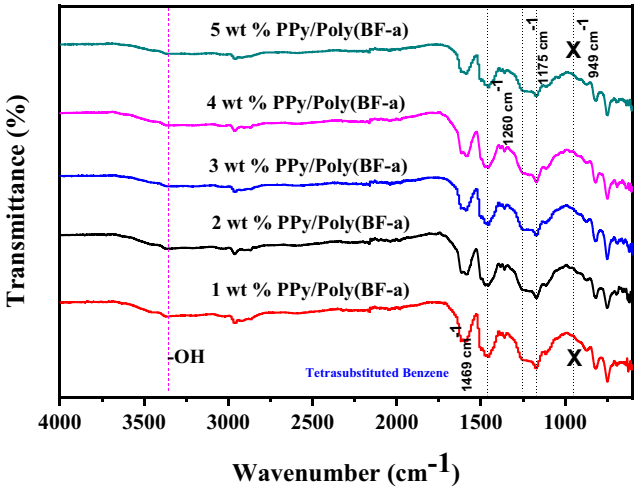

Fig. 5 FTIR spectra of PPy/poly(BF-a)

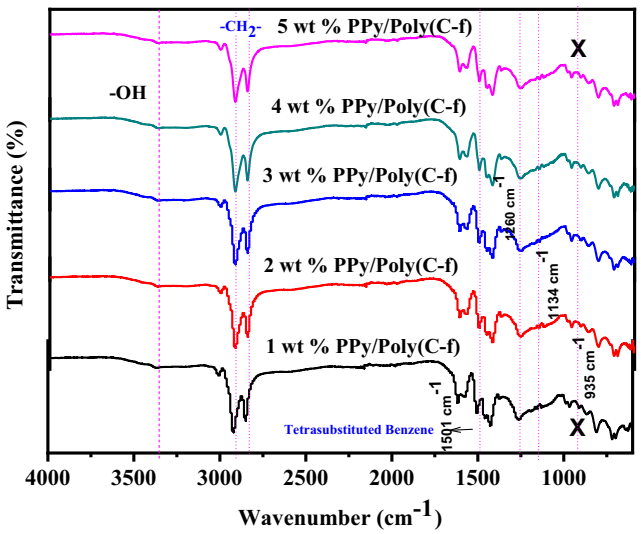

Fig. 4 FTIR spectra of PPy/poly(C-f)

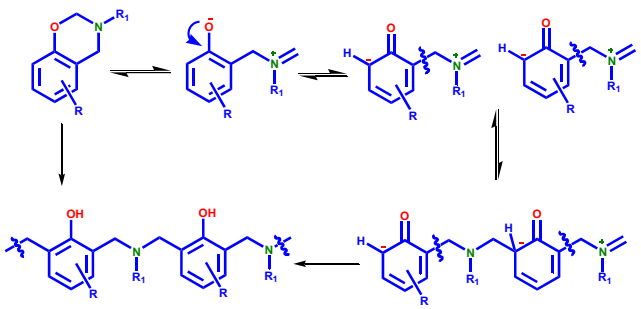

Scheme 2 General Curing mechanism of benzoxazines

Scheme 3 Mechanism for the catalytic activity of polypyrrole in curing benzoxazine

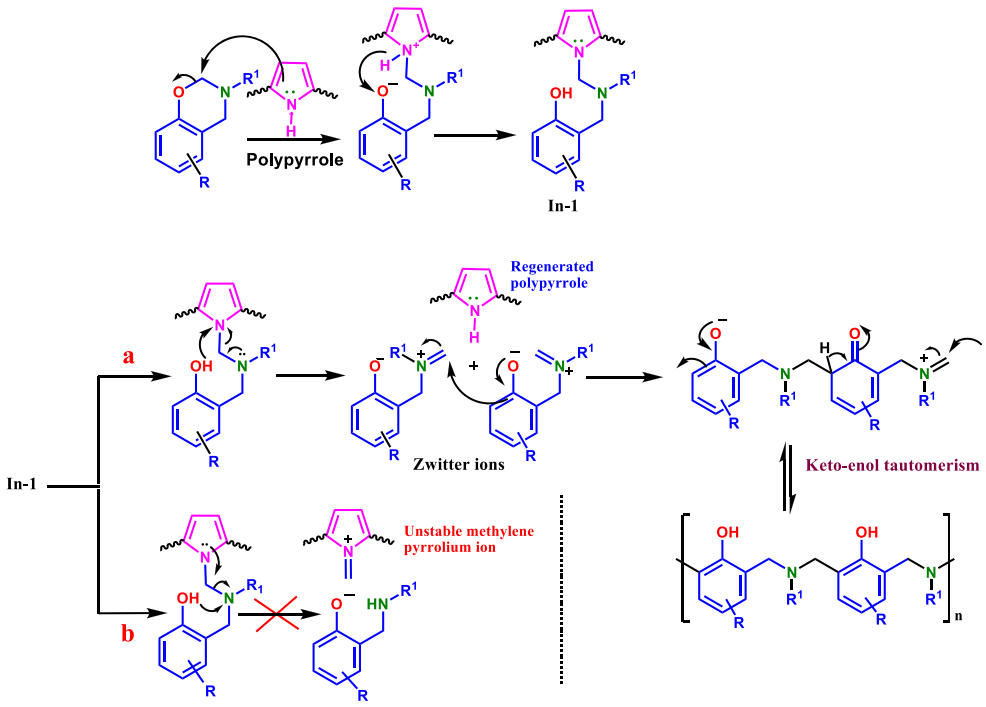

favoured interaction between PPy and benzoxazine through the pathway 'a' mechanism (Scheme 3), it is concluded that the PPy has catalytic activity similar to other amines. Further, to study the interaction between the PPy and polybenzoxazines, the microstructure and diffraction analysis were carried out and discussed subsequently.

Morphological analysis

The morphology of the prepared polypyrrole, neat poly(C-f) and neat poly(BF-a) was analyzed using SEM and the images obtained are presented in Fig. 6. The morphology of PPy was observed to be granular structured [30]. However, the cured C-F and BF-a matrices exhibit smooth surfaces representing to the brittle nature of the resulted polybenzoxazines [40, 41].

Further micrographs observed for PPy incorporated poly/(C-f) and poly(BF-a) are also presented in Fig. 7. The curing of both C-f and BF-a in the presence of 1 wt% PPy demonstrates no significant change in the morphology. The smooth surfaces were observed to retained even after the addition of 1 wt% PPy. On the other hand, considerable changes in the morphology of both poly(C-f) and poly(BF-a) matrices were observed with incorporation of higher amount of PPy. Thus, the morphologies of the poly(C-f) and poly(BF-a) in the presence of 2 wt% PPy are observed to be rough and irregular. The ring opening polymerization of benzoxazine rings were initiated on the granular surface of the PPy. Due to the interconnected linear network of polypyrrole, ring opening of the individual monomers are simultaneous initiated, which could results in rapid curing of monomers as discussed earlier in DSC. These phenomenon lead to the formation of PPy inter layered covered with poly(C-f) matrices over the surface [42]. Meanwhile, the interaction such as hydrogen bonding and π–π stacking between polypyrrole with furan and benzene rings of polybenzoxazines leads to the inter-layered morphology [18] (Scheme 1). Similarly, the morphologies of PPy/poly(BF-a) were also analysed. Here,

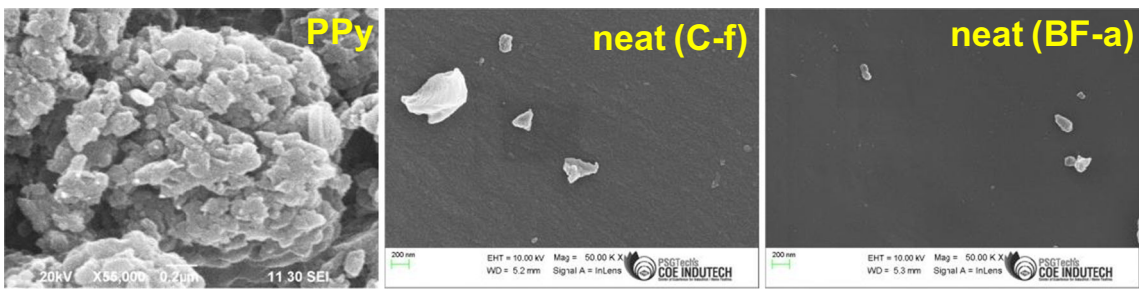

Fig. 6 SEM images of PPy, neat(C-f) and neat (BF-a)

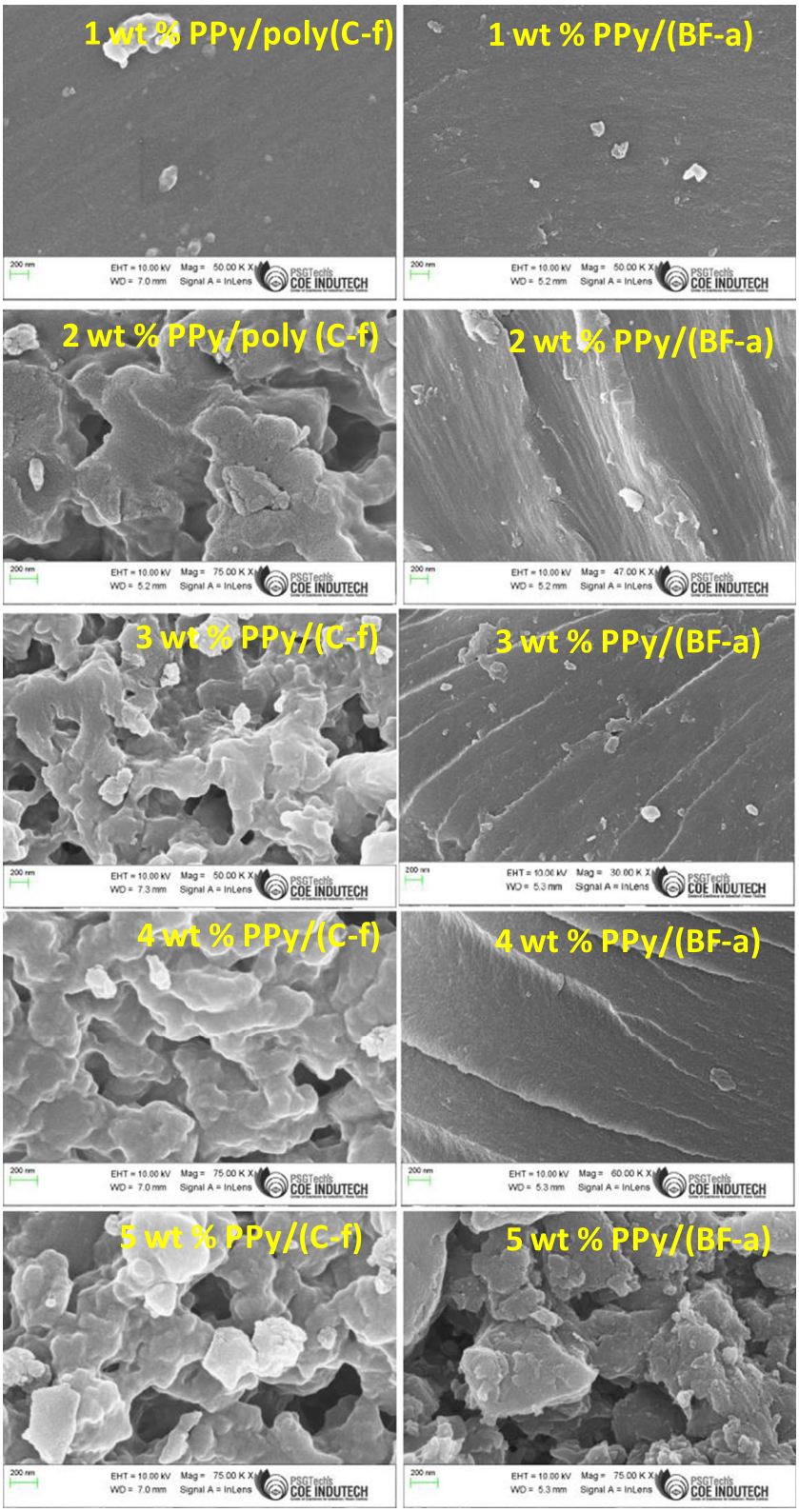

Fig. 7 SEM images of PPy/Poly(C-f) (left) and PPy/Poly(BF-a)(right)

except 5 wt% PPy/poly(BF-a) all other samples possess the rough surfaces. These observed morphologies are due to the rigid and brittle nature of bisphenol benzoxazine, and higher cross-linking nature of bi-functional BF-a compared to that of monofunctional C-f. However, at 5 wt% the interlayered PPy develops more free spaces and fractal morphologies, which might be due to the higher concentration of PPy.

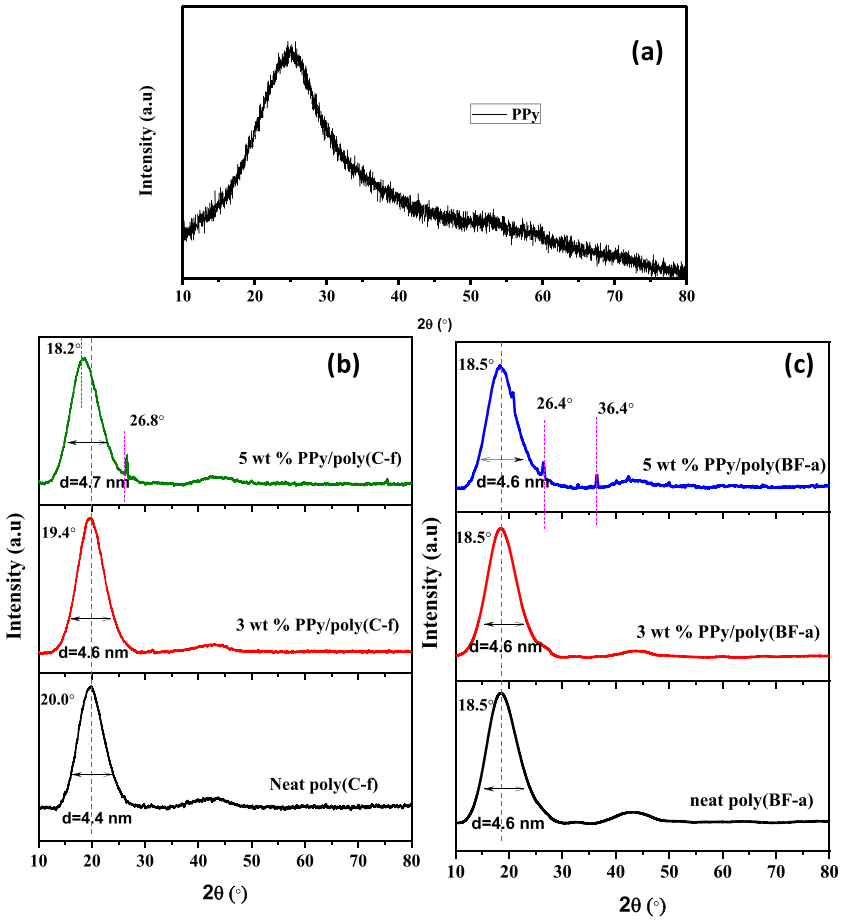

Fig. 8 XRD images of (**a**) PPy, **b** PPy/Poly(C-f) and **c** PPy/Poly(BF-a)

Further, in order to substantiate the formation of polybenzoxazines over the globular surface of PPy, the XRD analysis was carried out and presented in Fig. 8a-c. Figure 8a shows the XRD pattern of PPy with broad peak at 2θ = 26°, which clearly indicates the amorphous nature of the PPy [28, 43]. The XRD patterns of neat poly(C-f) shows a broad peak at 2θ = 20°, whereas the 3 wt% PPy/poly(C-f) and 5 wt% PPy/poly(C-f) show peak at 2θ = 19.4° and 18.2° respectively (Fig. 8b). It is significant to notice that the d-spacing values are also increased with increase in concentration of the PPy in addition to the chemical shift. At higher concentration of PPy, the formation of crystallinity is clearly attributed from the appearance of new peak at 2θ = 26.8°. Further, d spacing value of the neat poly(C-f) was observed to be 4.4 nm, whereas the 3 wt% PPy/poly(C-f) and 5 wt% PPy/poly(C-f) shows d spacing values as 4.6 and 4.7 nm respectively. This peak shifting and increase in d spacing might be due to the formation of interlayered polypyrrole over which the wrapping of polybenzoxazine matrices occurred with fractal structure arrangement [44, 45]. Further, the diffraction patterns of neat poly(BF-a) shows a broad peak at 2θ = 18.5°, whereas the 3 wt% PPy/poly(BF-a) and 5 wt% PPy/poly(BF-a) also show similar diffraction pattern at 2θ = 18.5° (Fig. 8c). The d spacing values are observed to be 4.6 nm for neat poly(BF-a), 3 wt% and 5 wt% PPy/poly(BF-a) respectively. Compared to poly(C-f) matrices, the poly(BF-a) shows no peak shifting and significant change in d spacing values. This might be due to the presence of high cross-linking and brittle nature of the bifunctional (BF-a) benzoxazines when compared to those of monofunctional (C-f) monomer. The observed results are also in accordance with microstructures observed in SEM.

Thermal property

Polybenzoxazine materials are widely used in industrial applications because of their high temperature resistance and flame retardant behaviour. However, compared to conventional bisphenol benzoxazines, the cardanol based polybenzoxazines possess inferior in their thermal stability. Hence, it is highly desirable to assess the influence of PPy in thermal behaviour of benzoxazines matrices. The thermal stability of the prepared PPy/poly(C-f) and PPy/poly(BF-a) matrices are studied using TGA and resulted thermograms are presented in Figs. 9 and 10 respectively along with the neat matrices. The thermal degradation temperature correspond to 1% and 10% weight loss are presented in Table 2 along with char yield obtained at 850 °C.

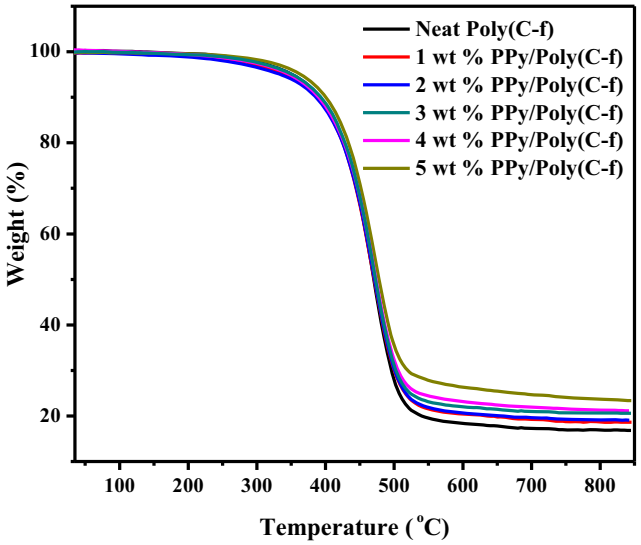

Fig. 9 TGA profile of neat (C-f) and PPy/Poly(C-f)

The neat poly(C-f) shows 1% weight loss at 183 °C, whereas the degradation of 1, 2, 3, 4, 5 wt% of PPy incorporated poly(C-f) matrices occurs at 211, 233, 247, 254 and 266 °C, respectively. In case of neat poly(BF-a) matrices, the 1% weight loss occurs at 352 °C, whereas the after addition of 1, 2, 3, 4 and 5 wt% PPy the 1% weight losses occurs at 361, 366, 370, 373 and 392 °C respectively. Similar behaviour is also observed with 10% weight losses for both matrices and the degradation temperatures observed are presented in Table 2. Thus, the incorporation of 1, 3, 5, 7, 10 wt% PPy enhances thermal stability to an appreciable extent. It is worthy to mention that the inter-layered PPy network present in the samples retards the heat transfer and thereby contributes to the enhancement of thermal stability similar to earlier reports [46–50]. Further, the char yield of the samples obtained at 850 °C is presented in Table 2. The char yields of neat

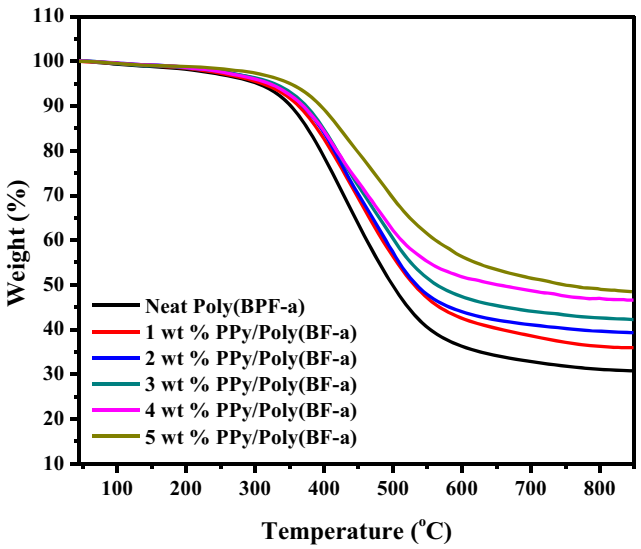

Fig. 10 TGA profile of neat (BF-a) and PPy/Poly(BF-a)

matrices of (C-F) and (BF-a) are observed to be 16.3% and 29.9% respectively, whereas the char yield of 5 wt% PPy/poly(C-f) and 5 wt% PPy/poly(BF-a) are observed as 23.5% and 48.5% respectively. In addition to restricting the heat transfer behaviour, the inter-layered polypyrrole contributes to the formation of higher volume of char upon heating. As a result, at high temperatures, the inter-layered polypyrrole along with polybenzoxazine matrices get carbonized, which in turn forms a cohesive carbon mass as residual chars [51].

Subsequently, the flame retardant behaviour of the PPy/poly(C-f) and PPy/poly(C-f) matrices are analyzed and compared with those of neat matrices using the Limiting Oxygen index (LOI) value. The LOI values were calculated using Van Krevelen and Hoftyzer relation (eq. 1) [46, 47].

$$\mathrm{LOI} = 17.5 + 0.4(\mathrm{CR}) \quad (1)$$

Here, CR is the percentage char yield of the sample remaining at 850 °C. It is experimentally proved that the materials having higher LOI values are flame retardant in nature. Generally, polymers with LOI values greater than 26 are ranked as excellent flame retardant material. The calculated LOI values are presented in Table 2. The char yields of both poly(C-f) and poly(BF-a) matrices are significantly increased with addition of PPy and thereby contributes for enhanced LOI values. Thus LOI values of poly(C-f) increased from 24.0 to 26.9 with the addition of 5% of PPy. In case of bisphenol-F based benzoxazines, the LOI values are increased from 29.9 to 36.9. The overall enhancement in LOI values might be due to the presence of thermally stable heterocyclic core of pyrrole ring inter-layered between the polybenzoxazine matrices as similar to the PPy doped epoxy matrices [51].

Dielectric property

Polybenzoxazines are used in microelectronics applications depending upon its dielectric properties [52–55]. The low dielectric materials are used as sealants, encapsulants, etc., whereas the high dielectric composites are used as anti-static coatings, electromagnetic interference shielding, embedded capacitors, gas sensors, and bipolar plates for polymer electrolyte fuel cells [56, 57]. Thus, based on the dielectric constant value of the polymers the end use was determined. Hence, it is worthy and highly desirable to study the dielectric behaviour of the polymer matrices.

Figures 11 and 12 illustrates the influence of PPy in the dielectric constant behaviour of poly(C-f) and poly(BF-a) respectively. Previously, PPy reinforced polymer matrices delivers high dielectric constant behaviour through the high polarisation behaviour and conductive nature of PPy [29, 38, 58, 59]. However, in the present case the value of dielectric constant decreases with increase in PPy. Interestingly, this reverse phenomenon noticed in the current case is attributed

Table 2 Thermal properties of PPy/Poly(C-f) and PPy/Poly (BF-a) hybrid matrices

Matrices	Thermal degradation (°C)			Char Residue (850 °C)	LOI
	T_1	T_{10}	T_{30}		
Neat Poly(C-f)	183	382	441	16.3	24.0
1 wt% PPy/Poly(C-f)	211	387	444	18.3	24.8
2 wt% PPy/Poly(C-f)	233	394	446	19.4	25.2
3 wt% PPy/Poly(C-f)	247	397	448	20.5	25.7
4 wt% PPy/Poly(C-f)	254	399	451	21.5	26.1
5 wt% PPy/Poly(C-f)	266	406	453	23.7	26.9
Neat Poly(BF-a)	136	352	425	31.0	29.9
1 wt% PPy/Poly(BF-a)	153	361	445	36.2	31.9
2 wt% PPy/Poly(BF-a)	162	366	449	39.9	33.4
3 wt% PPy/Poly(BF-a)	171	370	457	42.5	34.5
4 wt% PPy/Poly(BF-a)	177	373	464	46.5	36.1
5 wt% PPy/Poly(BF-a)	181	392	495	48.5	36.9

to the following reasons, i) low concentration of PPy which is below the percolation thresholds limit [60], ii) formation of inter-layered PPy network structure. As discussed in SEM and XRD, the stacked PPy in between the polymer matrices forms fractal structure, which in turn forms free space with air voids. These air voids, whose dielectric value (k = 1) participate actively and influences dielectric properties of both poly(C-f) and poly(BF-a) matrices as an insulating layer [61, 62]. Finally, due to inter-layered PPy with free space affords less interfacial interaction and reduces the dielectric constant. The formation of inter penetrated network of PPy through stacking was discussed earlier in XRD. It was observed from dielectric studies that the value of dielectric constant of neat poly(C-f) and poly(BF-a) matrices are 4.4 and 4.7 respectively. However, after incorporation of 5% PPy, the dielectric values of poly(C-f) and poly(BF-a) are found to be 3.34 and 3.83 respectively. In addition to decrement in cure temperature, the dielectric constant values are also reduced with the incorporation of PPy. Thus, dual functional behaviour of the PPy has been explored in the present investigation. This phenomenon is highly essential for microelectronic application in order to reduce the signal to noise ratio with high propagation [39, 63, 64].

Conclusions

Curing temperature of two different types of benzoxazines have been reduced significantly using conductive polypyrrole (PPy) as a catalyst. The catalytic behaviour of PPy was analysed using both synthetic and bio-based benzoxazines namely Bisphenol-F, aniline derived bifunctional (BF-a) and

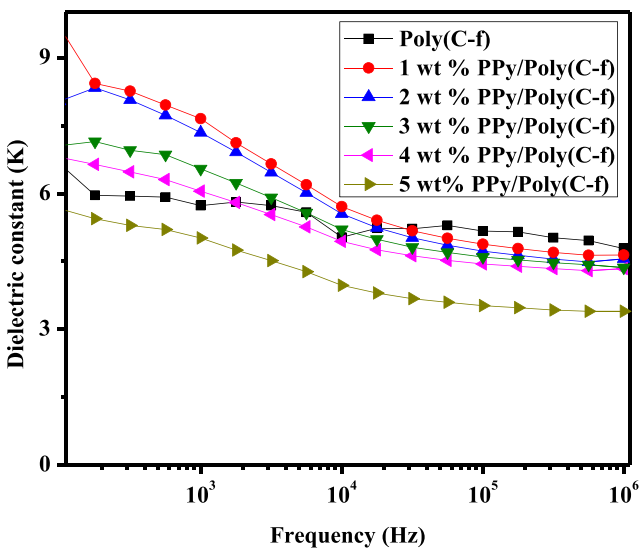

Fig. 11 Dielectric constant profile of neat (C-f) and PPy/poly(C-f)

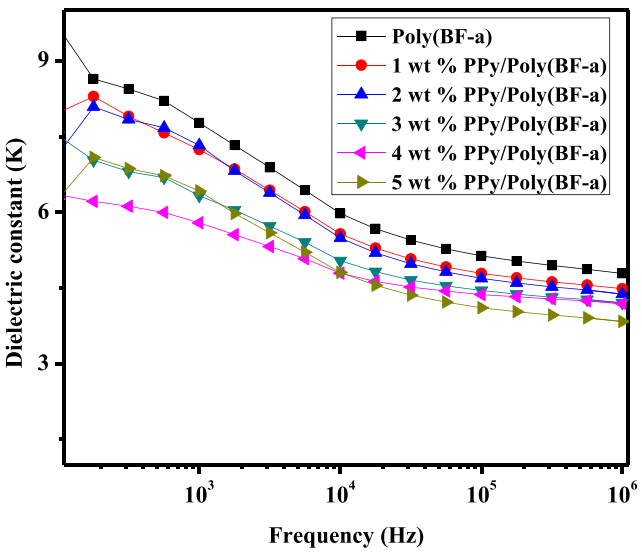

Fig. 12 Dielectric constant profile of neat (BF-a) and PPy/poly(BF-a)

bio-based cardanol, furfurylamine derived monofunctional (C-f) monomers, respectively. The curing temperature (Tp) of both C-f and BF-a are reduced to the similar extent of 60 °C. In addition, the possible reaction pathway including the mechanism is also proposed. The studies based on diffraction analysis and microstructure clearly demonstrates the formation of inter-layered structure of PPy wrapped with polybenzoxazines matrices. The generation of free space renders the low dielectric behaviour in the presence of 5 wt% PPy. Thus, the present work demonstrates the catalytic role of PPy to cure benzoxazine matrices in addition to the improvement of their thermal and dielectric behaviours.

Acknowledgments The authors thank the SERB, India (TAR/2019/000234) and PSG Management, Coimbatore, India for their financial support. The authors also thank SIF, VIT Vellore for providing NMR facility.

Compliance with ethical standards

Conflict of interest The authors have no conflict of interest.

References

1. Liao CS, Wang CF, Lin HC et al (2009) Fabrication of patterned superhydrophobic polybenzoxazine hybrid surfaces. Langmuir 25:3359–3362. https://doi.org/10.1021/la900176c
2. Liu J, Lu X, Xin Z, Zhou C (2013) Synthesis and surface properties of low surface free energy silane-functional polybenzoxazine films. Langmuir 29:411–416. https://doi.org/10.1021/la303730m
3. Qu L, Zhou C, Xin Z, Liu J (2012) Preparation and surface properties of fluorinated silane-functional polybenzoxazine films. Huagong Xuebao/CIESC J 63:1934–1942. https://doi.org/10.3969/j.issn.0438-1157.2012.06.041
4. Wen J, Wilkes GL (1996) Organic/inorganic hybrid network materials by the sol-gel approach. Chem Mater 8:1667–1681. https://doi.org/10.1021/cm9601143
5. Sawaryn C, Landfester K, Taden A (2011) Benzoxazine miniemulsions stabilized with multifunctional main-chain benzoxazine protective colloids. Macromolecules 44:5650–5658. https://doi.org/10.1021/ma200973g
6. Alhwaige AA, Agag T, Ishida H, Qutubuddin S (2013) Biobased chitosan/polybenzoxazine cross-linked films: preparation in aqueous media and synergistic improvements in thermal and mechanical properties. Biomacromolecules 14:1806–1815. https://doi.org/10.1021/bm4002014
7. Wang MW, Lin CH, Juang TY (2013) Steric hindrance control synthesis of primary amine-containing benzoxazines and properties of the resulting poly(benzoxazine imide) thermosetting films. Macromolecules 46:8853–8863. https://doi.org/10.1021/ma401756d
8. Pyun J, Matyjaszewski K (2001) [Chem.Mater 2001 Jeffry pyun] synthesis of Nanocomposite organic inorganic Hybrid.pdf. 3436–3448
9. Zhang K, Zhuang Q, Liu X et al (2013) A new benzoxazine containing benzoxazole-functionalized polyhedral oligomeric silsesquioxane and the corresponding polybenzoxazine nanocomposites. Macromolecules 46:2696–2704. https://doi.org/10.1021/ma400243t
10. Hanbeyoglu B, Kiskan B, Yagci Y (2013) Hydroxyl functional polybenzoxazine precursor as a versatile platform for post-polymer modifications. Macromolecules 46:8434–8440. https://doi.org/10.1021/ma401888g
11. Lin RC, Mohamed MG, Kuo SW (2017) Benzoxazine/Triphenylamine-based Dendrimers prepared through facile one-pot Mannich condensations. Macromol Rapid Commun 38:1–7. https://doi.org/10.1002/marc.201700251
12. Akkus B, Kiskan B, Yagci Y (2019) Counterion effect of amine salts on ring-opening polymerization of 1,3-Benzoxazines. Macromol Chem Phys 220:1–8. https://doi.org/10.1002/macp.201800268
13. Liu J, Agag T, Ishida H (2010) Main-chain benzoxazine oligomers: a new approach for resin transfer moldable neat benzoxazines for high performance applications. Polymer (Guildf) 51:5688–5694. https://doi.org/10.1016/J.POLYMER.2010.08.059
14. Liu J, Ishida H (2014) Anomalous isomeric effect on the properties of Bisphenol F-based Benzoxazines: toward the molecular Design for Higher Performance. Macromolecules 47:5682–5690. https://doi.org/10.1021/ma501294y
15. Ambrožič R, Šebenik U, Krajnc M (2015) Synthesis, curing kinetics, thermal and mechanical behavior of novel cardanol-based benzoxazines. Polymer (Guildf) 76:203–212. https://doi.org/10.1016/j.polymer.2015.08.065
16. Li S, Yan S, Yu J, Yu B (2011) Synthesis and characterization of new benzoxazine-based phenolic resins from renewable resources and the properties of their polymers. J Appl Polym Sci 122:2843–2848. https://doi.org/10.1002/app.34342
17. Wang J, Xu YZ, Fu YF, Liu XD (2016) Latent curing systems stabilized by reaction equilibrium in homogeneous mixtures of benzoxazine and amine. Sci Rep 6:1–7. https://doi.org/10.1038/srep38584
18. Zhang K, Tan X, Wang Y, Ishida H (2019) Unique self-catalyzed cationic ring-opening polymerization of a high performance deoxybenzoin-based 1,3-benzoxazine monomer. Polymer (Guildf) 168:8–15. https://doi.org/10.1016/j.polymer.2019.01.089
19. Liu C, Shen D, Sebastián RM et al (2013) Catalyst effects on the ring-opening polymerization of 1,3-benzoxazine and on the polymer structure. Polymer (Guildf) 54:2873–2878. https://doi.org/10.1016/j.polymer.2013.03.063
20. Zhang L, Mao J, Wang S et al (2017) Meta-phenylenediamine formaldehyde oligomer: a new accelerator for benzoxazine resin. React Funct Polym 121:51–57. https://doi.org/10.1016/j.reactfunctpolym.2017.10.020
21. Zong J, Ran Q (2019) Ring opening reaction of 3,4-Dihydro-2 *H*-1,3-Benzoxazine with amines at room temperature. ChemistrySelect 4:6687–6696. https://doi.org/10.1002/slct.201901447
22. Agag T, Arza CR, Maurer FHJ, Ishida H (2010) Primary amine-functional benzoxazine monomers and their use for amide-containing monomeric benzoxazines. Macromolecules 43:2748–2758. https://doi.org/10.1021/ma902556k
23. Sun J, Wei W, Xu Y et al (2015) A curing system of benzoxazine with amine: reactivity, reaction mechanism and material properties. RSC Adv. https://doi.org/10.1039/c4ra16582a
24. Li S, Zhao C, Gou H et al (2017) Synthesis and characterization of aniline-dimer-based electroactive benzoxazine and its polymer. RSC Adv 7:55796–55806. https://doi.org/10.1039/c7ra11349h
25. Kocaarslan A, Kiskan B, Yagci Y (2017) Ammonium salt catalyzed ring-opening polymerization of 1,3-benzoxazines. Polymer (Guildf) 122:340–346. https://doi.org/10.1016/j.polymer.2017.06.077
26. Agag T, Geiger S, Alhassan SM et al (2010) Low-viscosity polyether-based main-chain benzoxazine polymers: precursors for flexible thermosetting polymers. Macromolecules 43:7122–7127. https://doi.org/10.1021/ma1014337

27. Zhang K, Han L, Froimowicz P, Ishida H (2017) A smart latent catalyst containing o-Trifluoroacetamide functional Benzoxazine: precursor for low temperature formation of very high performance Polybenzoxazole with low dielectric constant and high thermal stability. Macromolecules 50:6552–6560. https://doi.org/10.1021/acs.macromol.7b00887
28. Liu Y-C, Chuang TC (2003) Synthesis and characterization of gold/Polypyrrole Core−Shell Nanocomposites and elemental gold nanoparticles based on the gold-containing Nanocomplexes prepared by electrochemical methods in aqueous solutions. J Phys Chem B 107:12383–12386. https://doi.org/10.1021/jp035680h
29. Barrau S, Demont P, Maraval C et al (2005) Glass transition temperature depression at the percolation threshold in carbon nanotube-epoxy resin and polypyrrole-epoxy resin composites. Macromol Rapid Commun 26:390–394. https://doi.org/10.1002/marc.200400515
30. Navale ST, Mane AT, Chougule MA et al (2014) Highly selective and sensitive room temperature NO2 gas sensor based on polypyrrole thin films. Synth Met 189:94–99. https://doi.org/10.1016/J.SYNTHMET.2014.01.002
31. Mane AT, Navale ST, Sen S et al (2015) Nitrogen dioxide (NO2) sensing performance of p-polypyrrole/n-tungsten oxide hybrid nanocomposites at room temperature. Org Electron 16:195–204. https://doi.org/10.1016/j.orgel.2014.10.045
32. Li SF, Huang WD (2011) Synthesis of new Benzoxazine from Cardanol-furfural resin and the properties of the corresponding polymer. Adv Mater Res 236–238:317–320. https://doi.org/10.4028/www.scientific.net/AMR.236-238.317
33. Hariharan A, Srinivasan K, Murthy C, Alagar M (2018) Synthesis and characterization of a novel class of low temperature cure Benzoxazines. J Polym Res 25:20–13. https://doi.org/10.1007/s10965-017-1423-0
34. Bonnaud L, Chollet B, Dumas L et al (2019) High-performance bio-based Benzoxazines from enzymatic synthesis of Diphenols. Macromol Chem Phys 220:1800312. https://doi.org/10.1002/macp.201800312
35. Wang MW, Jeng RJ, Lin CH (2015) Study on the ring-opening polymerization of Benzoxazine through multisubstituted Polybenzoxazine precursors. Macromolecules 48:530–535. https://doi.org/10.1021/ma502336j
36. Viet CX, Lan DNU, Hung TK (2018) Thermal curing of Benzoxazine blends from Cardanol- Furfurylamine and Diphenolic acid-aniline. IOP Conf Ser Mater Sci Eng 429:012068. https://doi.org/10.1088/1757-899X/429/1/012068
37. Devaraju S, Krishnadevi K, Sriharshitha S, Alagar M (2019) Design and development of environmentally friendly Polybenzoxazine–silica hybrid from renewable bio-resource. J Polym Environ 27:141–147. https://doi.org/10.1007/s10924-018-1327-z
38. Aradhana R, Mohanty S, Nayak SK (2019) Synergistic effect of polypyrrole and reduced graphene oxide on mechanical, electrical and thermal properties of epoxy adhesives. Polymer (Guildf) 166:215–228. https://doi.org/10.1016/j.polymer.2019.02.006
39. Zhang K, Yu X, Kuo SW (2019) Outstanding dielectric and thermal properties of main chain-type poly(benzoxazine-: co -imide- co -siloxane)-based cross-linked networks. Polym Chem 10:2387–2396. https://doi.org/10.1039/c9py00464e
40. Rajesh Kumar S, Dhanasekaran J, Krishna Mohan S (2015) Epoxy benzoxazine based ternary systems of improved thermo-mechanical behavior for structural composite applications. RSC Adv 5:3709–3719. https://doi.org/10.1039/c4ra10901e
41. Kumaresan I, Pichaimani P, Ellappan S, Paramasivam M (2018) Ceria doped mullite reinforced polybenzoxazine nanocomposites with improved UV-shielding and thermo-mechanical properties. Polym Compos 39:2073–2080. https://doi.org/10.1002/pc.24169
42. Pattanayak P, Pramanik N, Kumar P, Kundu PP (2018) Fabrication of cost-effective non-noble metal supported on conducting polymer composite such as copper/polypyrrole graphene oxide (Cu2O/PPy–GO) as an anode catalyst for methanol oxidation in DMFC. Int J Hydrog Energy 43:11505–11519. https://doi.org/10.1016/J.IJHYDENE.2017.04.300
43. Liu A, Li C, Bai H, Shi G (2010) Electrochemical deposition of polypyrrole/sulfonated graphene composite films. J Phys Chem C 114:22783–22789. https://doi.org/10.1021/jp108826e
44. Chen F, Xing Y, Wang Z et al (2016) Nanoscale Polydopamine (PDA) meets π–π interactions: an Interface-directed Coassembly approach for Mesoporous nanoparticles. Langmuir 32:12119–12128. https://doi.org/10.1021/acs.langmuir.6b03294
45. Sasi kumar R, Padmanathan N, Alagar M (2015) Design of hydrophobic polydimethylsiloxane and polybenzoxazine hybrids for interlayer low k dielectrics. New J Chem 39:3995–4008. https://doi.org/10.1039/C4NJ02188F
46. Kim SH, Jang SH, Byun SW et al (2003) Electrical properties and EMI shielding characteristics of polypyrrole-nylon 6 composite fabrics. J Appl Polym Sci 87:1969–1974. https://doi.org/10.1002/app.11566
47. Omastová M, Kosina S, Pionteck J et al (1996) Electrical properties and stability of polypyrrole containing conducting polymer composites. Synth Met 81:49–57. https://doi.org/10.1016/0379-6779(96)80228-1
48. Zhang T, Wang J, Feng T et al (2015) A novel high performance oxazine derivative: design of tetrafunctional monomer, step-wise ring-opening polymerization, improved thermal property and broadened processing window. Polym Chem. https://doi.org/10.1039/x0xx00000x
49. Lin RC, Kuo SW (2018) Well-defined benzoxazine/triphenylamine-based hyperbranched polymers with controlled degree of branching. RSC Adv 8:13592–13611. https://doi.org/10.1039/c8ra00506k
50. Mohamed MG, Hsiao CH, Luo F et al (2015) Multifunctional polybenzoxazine nanocomposites containing photoresponsive azobenzene units, catalytic carboxylic acid groups, and pyrene units capable of dispersing carbon nanotubes. RSC Adv 5:45201–45212. https://doi.org/10.1039/c5ra07983g
51. Zhang X, Yan X, Guo J et al (2015) Polypyrrole doped epoxy resin nanocomposites with enhanced mechanical properties and reduced flammability. J Mater Chem C 3:162–176. https://doi.org/10.1039/c4tc01978d
52. Ramdani N, Derradji M, Feng T et al (2015) Preparation and characterization of thermally-conductive silane-treated silicon nitride filled polybenzoxazine nanocomposites. Mater Lett 155:34–37. https://doi.org/10.1016/J.MATLET.2015.04.097
53. Hamerton I, Howlin BJ, Mitchell AL et al (2012) Systematic examination of thermal, mechanical and dielectrical properties of aromatic polybenzoxazines. React Funct Polym 72:736–744. https://doi.org/10.1016/J.REACTFUNCTPOLYM.2012.07.001
54. Chen S-HSW-A (2002) Microelectronic or optoelectronic package having a polybenzoxazine-based film as an underfill material. US20070117263A1
55. Zhang K, Yu X (2018) Catalyst-free and low-temperature Terpolymerization in a single-component Benzoxazine resin containing both Norbornene and acetylene functionalities. Macromolecules 51:6524–6533. https://doi.org/10.1021/acs.macromol.8b01558
56. Das-Gupta DK, Doughty K (1988) Polymer-ceramic composite materials with high dielectric constants. Thin Solid Films 158:93–105. https://doi.org/10.1016/0040-6090(88)90306-9
57. Cherney EA (2005) Silicone rubber dielectrics modified by inorganic fillers for outdoor high voltage insulation applications. IEEE

Trans Dielectr Electr Insul 1108–1115. https://doi.org/10.1109/TDEI.2005.1561790
58. Armelin E, Pla R, Liesa F et al (2008) Corrosion protection with polyaniline and polypyrrole as anticorrosive additives for epoxy paint. Corros Sci 50:721–728. https://doi.org/10.1016/j.corsci.2007.10.006
59. Kim BG, Kim YS, Kim YH et al (2016) Nano-scale insulation effect of polypyrrole/polyimide core-shell nanoparticles for dielectric composites. Compos Sci Technol 129:153–159. https://doi.org/10.1016/j.compscitech.2016.04.028
60. Martens HCF, Brom HB, Reedijk JA et al (1999) Dielectric study of polypyrrole/epoxy composites. Synth Met 102:1236–1237. https://doi.org/10.1016/S0379-6779(98)01434-9
61. Prabunathan P, Thennarasu P, Song JK, Alagar M (2017) Achieving low dielectric, surface free energy and UV shielding green nanocomposites: via reinforcing bio-silica aerogel with polybenzoxazine. New J Chem 41:5313–5321. https://doi.org/10.1039/c7nj00138j
62. Le TH, Kim Y, Yoon H (2017) Electrical and electrochemical properties of conducting polymers. Polymers (Basel) 9:150
63. Shih HK, Hsieh CC, Mohamed MG, Zhu CY, Kuo SW (2016) Ternary polybenzoxazine/POSS/SWCNT hybrid nanocomposites stabilized through supramolecular interactions. Soft Matter 12:1847–1858. https://doi.org/10.1039/c5sm02569a
64. Mohamed MG, Kuo SW (2019) Functional silica and carbon nanocomposites based on polybenzoxazines. Macromol Chem Phys 220:1–13. https://doi.org/10.1002/macp.201800306